Research Article
doi.org/10.1002/cbic.202100618

Selective Disruption of Survivin's Protein-Protein Interactions: A Supramolecular Approach Based on Guanidiniocarbonylpyrrole

Dennis Aschmann,[a] Cecilia Vallet,[b] Sunil K. Tripathi,[c] Yasser B. Ruiz-Blanco,[c] Max Brabender,[b] Carsten Schmuck[+],[a] Elsa Sanchez-Garcia,*[c] Shirley K. Knauer,*[b] and Michael Giese*[a]

Targeting specific protein binding sites to interfere with protein-protein interactions (PPIs) is crucial for the rational modulation of biologically relevant processes. Survivin, which is highly overexpressed in most cancer cells and considered to be a key player of carcinogenesis, features two functionally relevant binding sites. Here, we demonstrate selective disruption of the Survivin/Histone H3 or the Survivin/Crm1 interaction using a supramolecular approach. By rational design we identified two structurally related ligands ($\mathbf{L}_{NES}$ and $\mathbf{L}_{HIS}$), capable of selectively inhibiting these PPIs, leading to a reduction in cancer cell proliferation.

Protein-protein interactions (PPIs) are involved in nearly all cellular processes (e.g. cell proliferation, cell division, and programmed cell death) and are indispensable for human life.[1] They play critical roles in various pathological conditions such as cardiovascular diseases, neurodegeneration, and cancer.[2] Thus, PPIs provide an attractive target with massive therapeutic potential for the treatment of diseases.[3] The binding surfaces between proteins are, in most cases, large (1500–3000 Å^2) and involve many hydrophobic and polar interactions.[4] Additionally, such surfaces are usually flat, thus often lacking a defined binding pocket.[4a] Therefore, targeting PPIs with small molecules is very challenging, particularly as most proteins can interact with more than one binding partner involving different surface regions. Inhibiting one specific interaction and at the same time not influencing other biologically relevant processes is thus an ambitious endeavour. The cancer-relevant protein Survivin is upregulated in virtually all human cancers, but mostly absent in differentiated adult tissues.[5] Expression of Survivin is moreover associated with resistance against chemo- and radiotherapy and poor clinical outcome making it an attractive target for cancer therapy.[5,6] Unlike other cancer-related proteins, Survivin does not offer an active site to target, but its function is regulated by a dynamic interplay of PPIs with different interaction partners.[7]

The interaction between Survivin's nuclear export signal (NES) and the export receptor Crm1 ensures continuous transport into the cytoplasm, where Survivin acts as an inhibitor of apoptosis. On the other hand, by binding to Histone H3 at the early stages of mitosis, Survivin also fulfils its role as a member of the chromosomal passenger complex (CPC). To enable both PPIs, Survivin possesses distinct anionic hot spots that are surface-exposed and overlap with functionally relevant regions: The Histone H3 binding site ^{51}**E**P**D**LAQCFFCFK**EL**E**G**W**EP**D**DD**-PI**EE**HKKH^{80} and the Crm1 interaction site ^{89}VKKQF**EE**LTL^{98} (NES, anionic residues in bold). Recently, we reported a small molecule specifically addressing the Survivin Histone H3 site that successfully interfered with Histone H3 binding and consequently led to a reduction of cancer cell proliferation.[8]

Here, we show that subtle changes in the structure of guanidiniocarbonylpyrrole (GCP)-containing ligands allows to shift their specificity to either the NES or the Histone H3 binding site of Survivin. Notably, such change in the binding selectivity is achieved by rationally modifying the length of the linker and thus the spatial orientation of two of the four GCP motifs present in these ligands (Figure 1).

Guanidiniocarbonylpyrrole (GCP) is an arginine mimetic motif, which has a strong binding affinity with carboxylates and phosphates in aqueous solutions.[9] Under physiological conditions the GCP moiety is positively charged, leading to the formation of H-bonds enhanced ion pairs which are significantly stronger and more specific than binding by simple guanidinium cations as in arginine.[10] This was already shown by introducing

[a] D. Aschmann, Prof. Dr. C. Schmuck,[+] Prof.Dr. M. Giese
Department of Organic Chemistry
University of Duisburg-Essen
Universitätsstr. 7, 45141, Essen (Germany)
E-mail: michael.giese@uni-due.de
[b] Dr. C. Vallet, M. Brabender, Prof. Dr. S. K. Knauer
Department of Molecular Biology II
University of Duisburg-Essen
Universitätsstr. 5, 45141 Essen (Germany)
E-mail: shirley.knauer@uni-due.de
[c] Dr. S. K. Tripathi, Dr. Y. B. Ruiz-Blanco, Prof. Dr. E. Sanchez-Garcia
Computational Biochemistry
University of Duisburg-Essen
Universitätsstr. 2, 45117 Essen, Germany
E-mail: elsa.sanchez-garcia@uni-due.de
[+] Deceased August 2019.

Supporting information for this article is available on the WWW under https://doi.org/10.1002/cbic.202100618

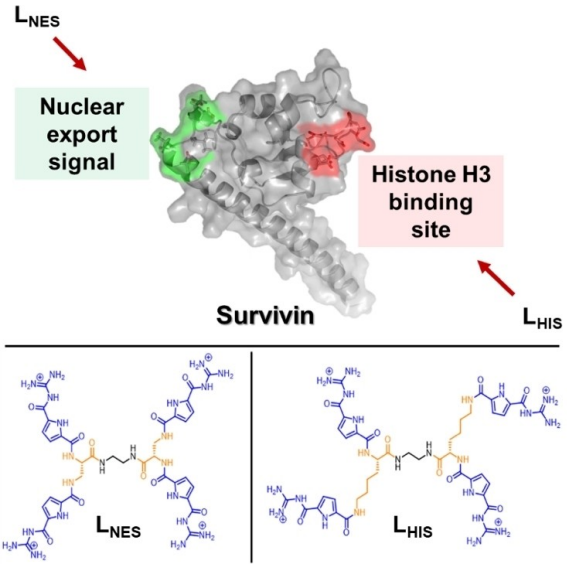

Figure 1. Schematic representation of one Survivin protomer with two biologically relevant PPI hot spots: The nuclear export signal (NES, green) and the Histone H3 binding site (red). Ligands L_{NES} and L_{HIS} were designed to target either the Histone H3 binding site (L_{HIS}) or the NES (L_{NES}). Guanidiniocarbonylpyrrole (GCP) groups are shown in blue and linker units in orange (bottom).

the GCP moiety into artificial transfection vectors and synthetic inhibitors for PPIs in cellular environments.[8–9,11] Now, we use the cationic GCP moiety to address negatively charged hot spots at the protein surface (e.g. glutamic acid and aspartic acid residues) of Survivin. Since the distances of the surface-exposed anionic amino acids differ between the NES and the Histone H3 binding site, the distance between the cationic GCP moieties is crucial for specific targeting to different binding sites. Based on this, we designed two GCP-ligands consisting of two symmetric peptide arms containing four GCP moieties (Figure 1; highlighted in blue). These two ligands (Figure 1; highlighted in orange) differ in linker length and rigidity (L_{NES} contains a short C2 linker, and for L_{HIS} a C5 linker (lysine) is introduced) allowing to address the different spatial orientations of anionic groups at the NES and the H3 binding site (Figure 1).

In the next step, the conformations of L_{HIS} and L_{NES} in solution and binding modes of the ligands to Survivin were investigated in detail. Therefore, we performed biomolecular modelling studies using previously reported coordinates of Survivin as starting point (see computational details).[7,12] The studies of the ligands and their Survivin complexes included classical molecular dynamics (MD) simulations, Gaussian accelerated MDs,[13] molecular docking,[14] and end-state binding free energy calculations using central limit free energy perturbation (CL-FEP), an unbiased FEP-based estimator.[15] Extensive blind docking calculations suggested that the NES region and the Histone H3 binding site are the two major binding regions for L_{NES} and L_{HIS} (Figure S5). L_{HIS} and L_{NES} showed opposite trends in their binding affinity to both sites, *i.e.* the NES is less favoured for L_{HIS} (12% of the docking poses) than for L_{NES} (28% of the docking poses). The Histone H3 binding site L_{HIS} (29% of the docking poses) is more favoured than L_{NES} (17% of the docking poses). This selectivity pattern was confirmed by site-specific binding free energy calculations (Table 1) and experimental assays.

Salt bridges are the main interactions stabilizing the binding of L_{HIS} and L_{NES} to Survivin thanks to the remarkable capability of the charged GCP moieties to form conserved ion pairs with carboxyl groups of aspartates and glutamates by means of bidentate H-bonds.[16]

Particularly the binding of L_{NES} to the NES shows very conserved bidentate H-bonds with D105, with occupancies (based on extended molecular dynamics simulations) of 94% and 93%. Such interactions stabilize the binding of one of the arms of L_{NES}, located at the crevice between the NES and the N-terminal tip of Survivin, which form the interface between protomers in the dimer of the native protein. Consequently, this binding mode considerably distorts the NES region. We note that, unlike L_{NES}, L_{HIS} does not interact with D105 of Survivin (Figure 2). However, both, L_{HIS} and L_{NES} interact with E94 (hydrogen bond occupancies of 39% and 42%, respectively), which is part of the NES region.[17] Thus, the conserved interaction between D105 and L_{NES} could be the major determinant of the increased affinity of L_{NES} towards the NES, compared to L_{HIS}.

The absolute binding free energies of L_{HIS} and L_{NES} in both binding sites were computed using the Central Limit Free

Table 1. Calculated binding free energy values for the Survivin complexes with the ligands L_{NES} and L_{HIS} bound to either the NES region or the Histone H3 binding site.

Complex	ΔG [kcal/mol]
L_{HIS} – **NES**	−4.0 ± 0.57
L_{HIS} – **Histone H3 binding site**	−7.3 ± 0.57
L_{NES} – **NES**	−13.7 ± 0.83
L_{NES} – **Histone H3 binding site**	−4.4 ± 0.68

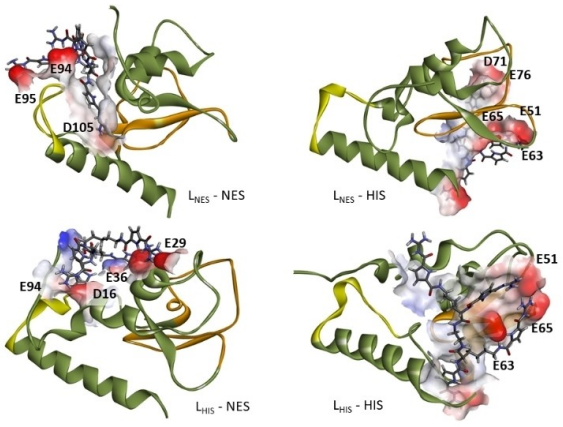

Figure 2. Schematic representation of the binding sites and interacting partners of L_{HIS} and L_{NES} with the NES (yellow) and the Histone H3 binding site (orange). The interacting residues are labelled in black. The molecular surface of the binding pocket is coloured by residue charge (red (negative) to blue (positive)). L_{HIS} and L_{NES} are shown in grey.

Energy Perturbation (CL-FEP) approach.[15] The results of these calculations show that L_{HIS} is favoured at the Histone H3 binding site by around 3 kcal/mol, while L_{NES} is favoured at the NES by more than 9 kcal/mol (see Table 1 and Supporting Information, Tables S1–S4, for details of the calculations).

To experimentally validate the promising results of the modelling studies, we synthesized our ligands L_{HIS} and L_{NES} as depicted in Scheme S1. Of note, all synthesis steps were accompanied by NMR (Figures S7 - S20) and mass spectrometry (Figures S21–S27). Having the final ligands in hand, we first used isothermal titration calorimetry (ITC) to assess their binding to Survivin (Figures S28 and S29). Indeed, a strong exothermic reaction profile was observed when Survivin was titrated to a solution of L_{HIS} or L_{NES}, indicating a binding event. The determination of free Gibbs energies ($T\Delta S$–$T\Delta S$) shows a slightly stronger binding of L_{NES} (−8.4 kcal/mol) than L_{HIS} (−7.6 kcal/mol) to Survivin, confirming the results of free energy calculations (Table 1).

The next step was to test whether the ligands influence Survivin's PPIs in a cellular environment. Therefore, we performed an *in situ* proximity ligation assay (PLA), which allows the visualization of protein-protein interactions within cells on an endogenous level. Briefly, primary antibodies bind to two potentially interacting targets, in our case Survivin and its export receptor Crm1 or Survivin and Histone H3. Respective secondary antibodies are conjugated to single-stranded oligonucleotide probes. If the two targets interact and are in close proximity (< 40 nm), the probes hybridize and form a circular DNA structure. When a DNA polymerase initiates rolling-circle amplification with fluorescent nucleotides, each interacting protein pair lights up as a fluorescent dot inside the cell (see also Supporting Information). The results clearly demonstrated that L_{NES} was able to reduce the number of interactions between Survivin and Crm1 by nearly 40%, while L_{HIS} had no significant effect on the Survivin-Crm1 interaction (Figure 3A).

In contrast, the interaction between Survivin and Histone H3 was decreased by 65% in L_{HIS}-treated cells during the early stages of mitosis (pro- and metaphase), while no significant effect could be observed in L_{NES}-treated cells (Figure 3B). This confirms a highly selective inhibition of both binding sites (Crm1 and Histone H3) by the respective ligands and is in good agreement with the calculations.

Since the interaction between Survivin and Crm1 is responsible for the active transport of Survivin from the nucleus into the cytoplasm, where the protein acts as an inhibitor of apoptosis, inhibition of the interaction should prevent Survivin's nuclear export inside the cell.[18] This was verified with a SRV100 biosensor assay (Figure 4) that allows the analysis of localization of the Survivin biosensor in the presence or absence of a potential Survivin-Crm1 inhibitor.[18c] The biosensor consists of a shortened version of Survivin (1–100), which still contains the NES that interacts with Crm1 (Figure 4A).

Furthermore, the biosensor contains two NLSs (nuclear localization signals) to ensure a nuclear localization of the biosensor when not actively exported by Crm1 as well as three FLAG-tags for immunofluorescence staining. Of note, the use of the biosensor is thus superior to transfection of fluorescently

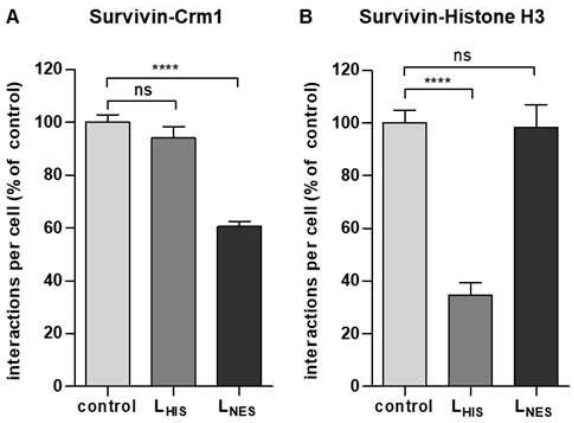

Figure 3. Selective inhibition of the Survivin-Crm1 and Survivin-Histone H3 interaction in Hela cells treated with 10 μM L_{NES} or L_{HIS}. A) *In situ* proximity ligation assay (PLA) showing the number of interactions between Survivin and Crm1 in HeLa cells with or without the addition of L_{NES} (10 μM) or L_{HIS} (10 μM). $n > 97$. B) PLA showing the number of interactions between Survivin and Histone H3 in HeLa cells arrested in the early stages of mitosis (pro- and metaphase) with or without the addition of L_{NES} (10 μM) or L_{HIS} (10 μM). $n > 30$. The error bars show the standard error of the mean, and only one of the two symmetrical error bars is depicted. Data were analysed by using the t test. Four asterisks (****) indicate a p value smaller than 0.0001.

tagged Survivin as the latter harbours no active NLS and does not allow the robust and quantitative analysis of nuclear accumulation after inhibitor treatment. HEK 293T cells were co-transfected with Crm1-GFP and the Survivin wildtype (SurvWT) biosensor with or without 10 μM L_{NES}. As a control, they were co-transfected with Crm1-GFP and the NESmut biosensor, containing a known export-deficient NES mutant of Survivin (L96A, L98A). This mutant cannot interact with Crm1 and mainly localizes to the nucleus of transfected cells. In our assay, it serves as a positive control for interference with Survivin's export activity.

To quantify the results, cells were assigned to one of three different groups: cells with a predominantly nuclear localization of the biosensor, cells with an evenly distributed biosensor and cells with a predominantly cytoplasmic localization of the biosensor. In 78% of cells transfected with SurvWT, the biosensor had a predominantly cytoplasmic localization, while it was evenly distributed in 19% of cells and predominantly nuclear in only 3% of cells. In L_{NES}-treated cells the proportion of cells with a cytoplasmic localization of the biosensor decreased to only 55%, while the biosensor was evenly distributed in 16% of cells and predominantly nuclear in 29% of cells. A reason for an only partial inhibition of Survivin's nuclear export could be that the biosensor, consisting of a shortened version of Survivin (1–100), lacks the residue D105, which was identified as one of the interaction sites of L_{NES} in the computational studies. In this experimental setup the interaction of the ligand with E94, which is part of the NES, might still allow sufficient binding. In control cells transfected with the NESmut biosensor, the localization was exclusively nuclear comparable to the situation where nuclear export of Survivin would be completely inhibited. Clearly, cellular application of a

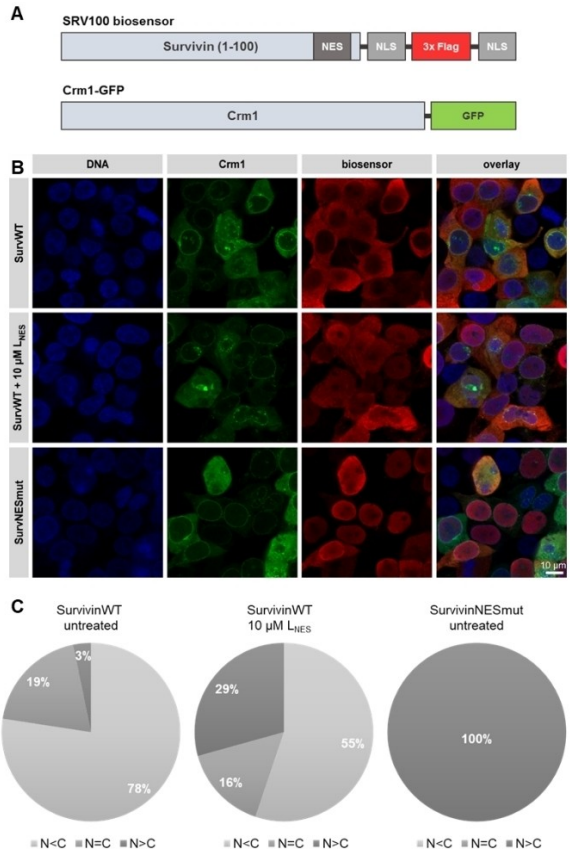

Figure 4. A) The SRV100 biosensor is composed of a shortened version of Survivin (1–100), two nuclear localization signals (NLS) and a 3×FLAG-tag. It was co-transfected with Crm1-GFP. B) Representative images of the SRV100 biosensor assay in HEK 293T cells. Cells were co-transfected with Crm1-GFP and the SurvWT or SurvNESmut biosensor. One of the SurvWT samples was additionally treated with 10 μM L_{NES} for 24 h before the samples were fixed and immune-stained. DNA is shown in blue, Crm1-GFP in green and the biosensor in red. C) Percentages of nucleocytoplasmic localization in SurvWT, SurvWT + L_{NES} and SurvNESmut samples. NESmut acts as positive control, containing a known export-deficient NES mutant of Survivin. N = nucleus, C = cytoplasm. N > 50.

chemical PPI inhibitor cannot be expected to achieve 100% inhibition like a specific genetic mutation. Nevertheless, a robust response of almost have of the biosensor-expressing cells serves as a reliable indicator of specific Survivin export inhibition in a cellular context.

The results confirm that L_{NES} is able at least partially to decrease the Crm1-mediated nuclear export of Survivin. To the best of our knowledge, L_{NES} is the first ligand which interferes with the Crm1-mediated nuclear export of Survivin inside the cell.

Since the PPI between Survivin and Histone H3 is essential for proper mitosis and the PPI between Survivin and Crm1 is crucial for Survivin to fulfil its role as an inhibitor of apoptosis, an interference with these PPIs should lead to decreased cell proliferation and viability. We thus quantified the inhibition effect of both ligands on cell proliferation by performing cell proliferation assays in different types of cancer cells: HeLa cells that are originating from cervical cancer, A549 cells as a model for lung cancer, MDA-MB-231 cells derived from breast cancer and HCT 116 cells that originate from colon cancer. Indeed, both L_{NES} and L_{HIS}, were able to inhibit cancer cell proliferation in a concentration-dependent manner. Both ligands had a strong effect on cell proliferation in A549 cells, where L_{NES} was able to decrease cell viability by almost 50% at a concentration of only 10 μM and by 66% at a concentration of 50 μM (Figure 5B).

L_{HIS} had similar effects and decreased cell viability by 69% at a concentration of 50 μM. L_{HIS} had a stronger impact on cell proliferation than L_{NES}. The former was able to decrease cancer cell proliferation by up to 80% in HCT 116 at a concentration of 100 μM (76% in HeLa cells and 63% in MDA-MB-231 and A549 cells). At this concentration L_{NES} decreased cell proliferation by 32% in HeLa cells, 25% in HCT 116 cells, 44% in MDA-MB-231 cells and 59% in A549 cells. The more prominent effect of L_{HIS} can be attributed to the fact that this ligand more directly interferes with cell proliferation, while L_{NES} mainly affects Survivin's export from the nucleus in interphase cells and thereby its anti-apoptotic function that is more indirect. Of note, especially A549 lung cancer cells showed an increased sensitivity towards our compounds. Indeed, Survivin has been reported to be associated with the development of drug resistance and to be involved in the progression of non-small

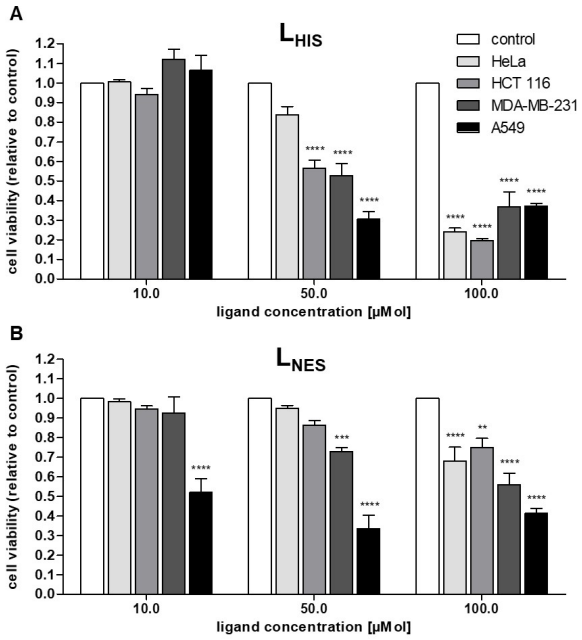

Figure 5. L_{HIS} and L_{NES} treatment leads to a concentration-dependent inhibition of cell proliferation in different types of cancer cells. HeLa, A549, MDA-MB-231 and HCT 116 cells were treated with different concentrations of L_{HIS} (A), L_{NES} (B) or the respective amounts of DMSO (control) and incubated for 72 h before cell proliferation was measured using the CellTiter 96® AQueous One Cell Proliferation Assay (Promega). The absorbance (490 nm) values of the samples were subtracted by a medium only measurement and normalized to the respective control. N = 3. The error bars show the standard error of the mean. Data were analysed by a 2way ANOVA test followed by a Bonferroni multiple comparisons test to compare each cell line to the respective control (white column). Two asterisks (**) indicate a p value smaller than 0.01. Three asterisks (***) indicate a p value smaller than 0.001. Four asterisks (****) indicate a p value smaller than 0.0001.

cell lung cancer.[19] As such, lung cancer cells might be indeed more dependent on Survivin and thus also more sensitive towards its inhibition. However, this should be investigated in more detail in future studies.

In summary, based on structural analysis and computational modelling, we identified two ligands (L_{NES} and L_{HIS}) that selectively inhibit different biologically relevant PPIs of Survivin to partner proteins (Histone H3 and Crm1). Accurate binding free energy calculations with CL-FEP confirm a preferential binding of L_{NES} to Survivin's NES compared to L_{HIS}, which is in direct agreement with experimental results. Accordingly, the binding free energy calculations also hind towards a stronger binding of L_{HIS} to Survivin's Histone H3 binding site with respect to L_{NES}. The ability of the ligands to distinguish between the Histone H3 and Crm1 binding site leading to a selective inhibition of only one PPI was shown via proximity ligation assay (PLA). Using a biosensor assay we proved that L_{NES} is the first known ligand able to reduce Survivin's nuclear export activity in a cellular context. We show that L_{NES} and L_{HIS} are both able to inhibit two cancer-relevant PPIs of Survivin, with a consequently reduced cell proliferation in different cancer cell lines.

Further studies will focus on the combination of the Histone H3 binding sequence with the recently reported artificial Histone H3 binder[7] to cover a larger area of the binding site. This should enable us to improve the binding affinity as well as the inhibitory potential of the ligands.

Acknowledgements

This work was supported by the collaborative research centre 1093 (CRC 1093) funded by the German Research Foundation (DFG), subprojects A01, A08 and B05. E.S.-G. was supported by the DFG under Germany's Excellence Strategy - EXC 2033-390677874 – RESOLV. E.S.-G. also acknowledges the support of the Boehringer Ingelheim Foundation (Plus-3 Program). E.S.-G. acknowledges the computational support by the DFG (Projektnummer: 436586093) and the supercomputer magnitUDE of the University of Duisburg-Essen. Microscopic analyses were performed in collaboration with the Imaging Centre Campus Essen (ICCE). We thank the group of Jose A. Rodríguez for providing the plasmids for the biosensor assay. M.G. thanks the Professor-Werdelmann Foundation for generous financial support. Open Access funding enabled and organized by Projekt DEAL.

Conflict of Interest

The authors declare no conflict of interest.

Data Availability Statement

The data that support the findings of this study are available on request from the corresponding author. The data are not publicly available due to privacy or ethical restrictions.

Keywords: cancer · CL-FEP · molecular recognition · supramolecular chemistry · survivin

[1] A. J. Wilson, *Chem. Soc. Rev.* **2009**, *38*, 3289–3300.
[2] a) E. Sijbesma, E. Visser, K. Plitzko, P. Thiel, L.-G. Milroy, M. Kaiser, L. Brunsveld, C. Ottmann, *Nat. Commun.* **2020**, *11*, 3954; b) O. Keskin, N. Tuncbag, A. Gursoy, *Chem. Rev.* **2016**, *116*, 4884–4909; c) D. C. Fry, L. T. Vassilev, *J. Mol. Med.* **2005**, *83*, 955–963.
[3] A. Barnard, K. Long, H. L. Martin, J. A. Miles, T. A. Edwards, D. C. Tomlinson, A. Macdonald, A. J. Wilson, *Angew. Chem. Int. Ed.* **2015**, *54*, 2960–2965; *Angew. Chem.* **2015**, *127*, 3003–3008.
[4] a) M. R. Arkin, Y. Tang, J. A. Wells, *Chem. Biol.* **2014**, *21*, 1102–1114; b) H. Hwang, T. Vreven, J. Janin, Z. Weng, *Proteins* **2010**, *78*, 3111–3114; c) J. C. Fuller, N. J. Burgoyne, R. M. Jackson, *Drug Discovery Today* **2009**, *14*, 155–161.
[5] F. Shojaei, F. Yazdani-Nafchi, M. Banitalebi-Dehkordi, M. Chehelgerdi, M. Khorramian-Ghahfarokhi, *Eur. J. Cancer* **2019**, *28*, 365–372.
[6] a) A. Meiners, S. Bäcker, I. Hadrović, C. Heid, C. Beuck, Y. B. Ruiz-Blanco, J. Mieres-Perez, M. Pörschke, J.-N. Grad, C. Vallet, D. Hoffmann, P. Bayer, E. Sánchez-García, T. Schrader, S. K. Knauer, *Nat. Commun.* **2021**, *12*, 1505; b) D. Martínez-García, N. Manero-Rupérez, R. Quesada, L. Korrodi-Gregório, V. Soto-Cerrato, *Med. Res. Rev.* **2019**, *39*, 887–909; c) F. Li, G. Ambrosini, E. Y. Chu, J. Plescia, S. Tognin, P. C. Marchisio, D. C. Altieri, *Nature* **1998**, *396*, 580–584.
[7] a) S. P. Wheatley, D. C. Altieri, *J. Cell Sci.* **2019**, *132*; b) M. A. Verdecia, H.-k. Huang, E. Dutil, D. A. Kaiser, T. Hunter, J. P. Noel, *Nat. Struct. Biol.* **2000**, *7*, 602–608; c) C. Sun, D. Nettesheim, Z. Liu, E. T. Olejniczak, *Biochemistry* **2005**, *44*, 11–17.
[8] C. Vallet, D. Aschmann, C. Beuck, M. Killa, A. Meiners, M. Mertel, M. Ehlers, P. Bayer, C. Schmuck, M. Giese, S. K. Knauer, *Angew. Chem. Int. Ed.* **2020**, *59*, 5567–5571; *Angew. Chem.* **2020**, *132*, 5614–5619.
[9] M. Li, S. Mosel, S. K. Knauer, C. Schmuck, *Org. Biomol. Chem.* **2018**, *16*, 2312–2317.
[10] L. Bartsch, M. Bartel, A. Gigante, J. Iglesias-Fernández, Y. B. Ruiz-Blanco, C. Beuck, J. Briels, N. Toetsch, P. Bayer, E. Sanchez-Garcia, C. Ottmann, C. Schmuck, *ChemBioChem* **2019**, *20*, 2921–2926.
[11] J. Matić, F. Šupljika, T. Tandarić, M. Dukši, P. Piotrowski, R. Vianello, A. Brozovic, I. Piantanida, C. Schmuck, M. R. Stojković, *Int. J. Biol. Macromol.* **2019**, *134*, 422–434.
[12] H. M. Berman, J. Westbrook, Z. Feng, G. Gilliland, T. N. Bhat, H. Weissig, I. N. Shindyalov, P. E. Bourne, *Nucleic Acids Res.* **2000**, *28*, 235–242.
[13] a) Y. Miao, V. A. Feher, J. A. McCammon, *J. Chem. Theory Comput.* **2015**, *11*, 3584–3595; b) W. Humphrey, A. Dalke, K. Schulten, *J. Mol. Graphics* **1996**, *14*, 33–38, 27–38; c) J. C. Phillips, R. Braun, W. Wang, J. Gumbart, E. Tajkhorshid, E. Villa, C. Chipot, R. D. Skeel, L. Kalé, K. Schulten, *J. Comput. Chem.* **2005**, *26*, 1781–1802.
[14] a) H. Zhao, A. Caflisch, *Bioorg. Med. Chem. Lett.* **2013**, *23*, 5721–5726; b) N. Zhang, H. Zhao, *Bioorg. Med. Chem. Lett.* **2016**, *26*, 3594–3597.
[15] Y. B. Ruiz-Blanco, E. Sanchez-Garcia, *J. Chem. Theory Comput.* **2020**, *16*, 1396–1410.
[16] J. Hatai, C. Schmuck, *Acc. Chem. Res.* **2019**, *52*, 1709–1720.
[17] R. H. Stauber, W. Mann, S. K. Knauer, *Cancer Res.* **2007**, *67*, 5999–6002.
[18] a) J. S. Murley, J. L. Arbiser, R. R. Weichselbaum, D. J. Grdina, *Free Radical Biol. Med.* **2018**, *123*, 39–52; b) J. A. Rodríguez, S. W. Span, C. G. M. Ferreira, F. A. E. Kruyt, G. Giaccone, *Exp. Cell Res.* **2002**, *275*, 44–53; c) I. García-Santisteban, I. Arregi, M. Alonso-Mariño, M. A. Urbaneja, J. J. Garcia-Vallejo, S. Bañuelos, J. A. Rodríguez, *Cell. Mol. Life Sci.* **2016**, *73*, 4685–4699.
[19] a) C. Zhou, Y. Zhu, B. Lu, W. Zhao, X. Zhao, *Oncol. Lett.* **2018**, *16*, 5466–5472; b) Y. Chen, X. Wang, W. Li, H. Zhang, C. Zhao, Y. Li, Z. Wang, C. Chen, *Anat. Rec.* **2011**, *294*, 774–780.

Manuscript received: November 9, 2021
Revised manuscript received: December 9, 2021
Version of record online: January 18, 2022